Video-Based Monitoring of Pedestrian Movements at Signalized Intersections

Yegor Malinovskiy, Yao-Jan Wu, and Yinhai Wang

Pedestrian and cyclist crossing characteristics are important for the design of urban intersections and signalized crossings. Parameters such as waiting time, crossing time, and arrival rate are key variables for describing pedestrian characteristics and improving crossing designs and signal timing plans. Manually collecting such data is often extremely labor intensive. Therefore, an automated computer-vision-based approach is introduced for collecting these parameters in real time with ordinary video cameras. Broadly defined pedestrian objects, including bicyclists and other nonmotorized modes, are extracted by means of the background subtraction technique and tracked through an inherent cost characteristic function in conjunction with an α-β-filter. The waiting-zone concept introduced helps provide robust pedestrian tracking initialization and parameter extraction. The proposed approach is implemented in a pedestrian tracking (PedTrack) system by using Microsoft Visual C++. Tested with real video data from three study sites, this system was proved to be effective and about 80% of pedestrian crossing events were successfully detected. PedTrack shows the potential to be a great data collection tool for nonmotorized object movements at intersections.

Pedestrian and cyclist behavior dictates the design of numerous facilities, including urban intersections, as stated in the Transportation Equity Act for the 21st Century (TEA-21) (*1*). The need for data on nonmotorized traffic was highlighted in a recent report by the Bureau of Transportation Statistics (*2*). This report ranks information regarding the number of bicyclists and pedestrians by facility or geographic area as a high priority but notes the sparseness of available data. Much work has been done in the field of pedestrian and cyclist behavior (*3, 4*). Nevertheless, most of the data collection techniques rely on labor-intensive manual operations. In the case of large and widespread data set collection, manual methods remain fairly impractical and expensive.

Automatic detection and tracking of pedestrians and cyclists is still a largely open question. In terms of transportation applications, much work has been done for motorized vehicle detection and tracking (*5–9*). However, bicycle and pedestrian tracking is substantially different from automobile detection and often much more intricate. One of the differences is the freedom of motion that pedestrians and cyclists have with respect to motorized vehicles. Pedestrians and bicyclists are often not constrained by lane markings and prespecified movements. The relatively complicated inner motion of humans compared with the rigidly connected components of a vehicle is yet another complication. Many practical locations contain mixed modes of transit, resulting in further difficulties. A significant problem arises as the smaller objects, such as pedestrians and bicyclists, disappear behind the larger objects that are of no interest, resulting in frequent occlusions. Total occlusions are defined as the complete disappearance of one object behind a static element in the scene or another object.

Numerous automatic remote-sensing technologies have been implemented for intelligent transportation system applications in recent years. Although mostly vehicle-oriented, these technologies are primarily based on inductance, electromagnetic, microwave, infrared, video, or sonic signal interpretation. A recent study funded by FHWA (*10*) reviews a comprehensive list of available bicycle and pedestrian detection systems, but none of them offers complete tracking capabilities for collection of data on pedestrian and bicycle movement. The lack of practical systems for nonmotorized transport data collection motivates further research and development of pedestrian and bicycle detection technologies. Several approaches that use infrared sensors have been attempted with encouraging results (*11, 12*), yet the relatively high cost, narrow focus area, and mounting restrictions of infrared sensors make video-imaging techniques comparatively appealing. Video information is already available in many urban intersection locations from surveillance cameras, and temporary cameras can be easily mounted on or in nearby structures for data collection purposes.

An automated computer-vision-based approach for real-time pedestrian and cyclist detection and tracking with ordinary video cameras is introduced here. Currently, the scope of this research is set to daylight conditions in fair weather with good visibility since these conditions are the most relevant for pedestrians and bicyclists. Nighttime and bad weather conditions associated with poor visibility are not considered. The proposed approach significantly enhances the pedestrian tracking (PedTrack) system, first developed at the University of Washington Smart Transportation Applications and Research Laboratory (STAR Lab) in 2006 (*13*). PedTrack has been modified and enhanced to track and record pedestrian and cyclist movements at intersections. Three pedestrian parameters that describe a complete crossing event—waiting time, crossing time, and arrival time—are now automatically recorded for pedestrians appearing in live or stored video samples. These pedestrian parameters can also be retrieved and further analyzed to demonstrate the characteristics of pedestrian crossing movements at different intersections.

LITERATURE REVIEW

Video-based pedestrian and cyclist detection and tracking is a sophisticated field with many open questions. Numerous algorithms and techniques have been proposed. A feature-based algorithm was

Department of Civil and Environmental Engineering, Box 352700, University of Washington, Seattle, WA 98195-2700. Corresponding author: Y.-J. Wu, aojan@u.washington.edu.

Transportation Research Record: Journal of the Transportation Research Board, No. 2073, Transportation Research Board of the National Academies, Washington, D.C., 2008, pp. 11–17.
DOI: 10.3141/2073-02

implemented by Abramson and Steux (*14*). Learning of the features is done by using AdaBoost and a genetic-like algorithm. Although it provided fairly good performance, the algorithm is complicated and cannot be executed in real time on typical current computing devices. Satoh et al. (*15*) proposed a color-based probabilistic tracking method. However, the method may not always be practical since a significant portion of deployed surveillance cameras are still monocolor cameras. Point-feature detection and tracking techniques, such as the Harris or SUSAN corner detector (*16*), are promising techniques, since they are not reliant on background image quality and an extensive sample library. Nevertheless, these point-feature detectors are best suited to the tracking of rigid objects, such as vehicles, when the structural relationships between the points remain constant.

Pattern matching, as described by Munder and Gavrila (*17*), requires an extensive library of positive and negative samples in order to train the algorithm to recognize desired objects. Computation cost is also a serious concern for pattern-matching algorithms. The larger and more complete the library, the longer the matching process takes, and thus the process may not be performed in real time. In a recent study, Gavrila and Munder (*18*) presented a robust system combining shape-based and texture-based tracking algorithms. This system worked well as a driving assistance method. In the current study, background subtraction, a region-based approach, is used, since the intended applications typically maintain a stable background and the method is very common and straightforward for real-time applications, as was demonstrated by Zhang et al. and Zheng et al. (*5, 19*).

Regardless of the approach used, object tracking typically involves three steps: acquisition of moving objects, tracking, and classification (*20, 21*). Acquisition of moving objects can be done through a number of techniques, most of which focus on the comparison of either consequent frames or a derived background image with the current frame. Once the objects are acquired, tracking them through a complicated environment can be difficult because of occlusions and inconsistency in obtaining the same object throughout a sequence of frames (*22*). A Kalman filter is often used to clean the inconsistencies involved with tracking. The Kalman filter, however, is computationally expensive, and Blackman (*22*) suggests the use of an α-β-filter as a lighter alternative. Classification can occur before or after tracking, depending on the approach used. Static approaches that rely on inherent characteristics of the objects can classify them without path analysis (*23*). Harmonic-motion approaches to pedestrian tracking rely on some prior history of the object being tracked, which is not always available if the object is motionless, for example, a pedestrian waiting to cross.

There are still numerous challenges in pedestrian detection and tracking applications. The studies mentioned help guide efforts in further exploration of this field.

METHODOLOGY

The approach used to obtain pedestrian and bicyclist objects is based on previous work by Malinovskiy et al. with PedTrack (*13*). Since then, significant improvements and modifications have been made, including a broader orientation toward nonpedestrian objects, such as bicyclists and people boarding vehicles, by using less restrictive size and proportion characteristics. This revision allows for multimode analysis, as will be shown in the section on results. Therefore, the term "pedestrian" hereafter refers to not only regular pedestrian objects but also bicyclist and boarding objects for simplicity. In the following section the PedTrack system introduced in earlier work is reviewed. Improvements made to the original algorithm follow, along with the application-specific configurations introduced.

PedTrack Review

As in PedTrack, the approach here begins with simple background subtraction to extract foreground objects. As potential pedestrian objects are determined by their characteristics, such as size and proportion, an inherent cost function is adopted to track subsequent potential objects on the basis of their attributes of size, height, width, and grayscale color distribution. Occlusions are dealt with by watching and reasoning through splitting and merging. When two objects merge, a composite object is created and tracked as one. When an object splits, an attempt is made to recognize the resulting smaller objects as those that merged earlier to create the larger object. Finally, the output is shown as the trajectory of each successful candidate tracked. The details of the PedTrack algorithm can be found elsewhere (*13*) and are summarized in Figure 1.

Object Tracking

For most unobstructed angles of overhead observation, PedTrack is fairly robust. Failures arise when the scene becomes complicated, and pedestrians are occluded frequently by other foreground objects, such as wires and utility posts. As mentioned earlier, occlusion problems are tough challenges for image processing. In order

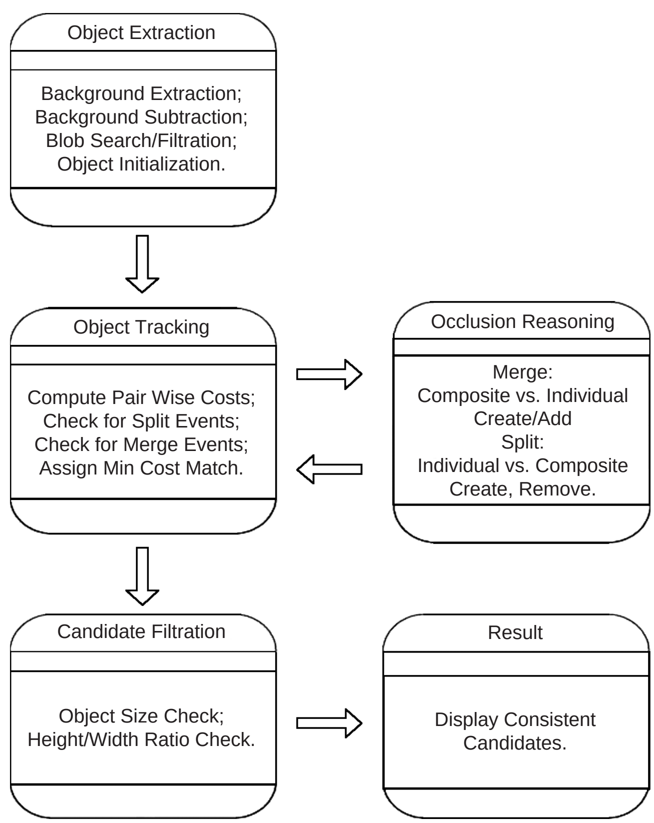

FIGURE 1 Review of basic PedTrack algorithm.

to handle these issues, a filter mechanism is incorporated into the PedTrack system. An α-β-filter was chosen since it is easy to implement and quick to compute because of its fixed parameters for filter gains. In this implementation, every single coordinate output is smoothed or predicted by this filter. The following equations show an example of how the filter handles output data points in the x-direction (*22*):

$$x_s(k) = \hat{x}(k|k) = x_p(k) + \alpha_x\left[x_o(k) - x_p(k)\right] \tag{1}$$

$$v_{sx}(k) = \hat{\dot{x}}(k|k) = v_{sx}(k-1) + \frac{\beta_x}{qT}\left[x_o(k) - x_p(k)\right] \tag{2}$$

$$x_p(k+1) = \hat{x}(k+1|k) = x_s(k) + T \cdot v_{sx}(k) \tag{3}$$

where

$x_o(k)$ = observed target position in x-direction at kth frame,
$x_p(k)$ = predicted target position in x-direction at kth frame,
$x_s(k)$ = smoothed target position in x-direction at kth frame,
$v_{sx}(k)$ = smoothed target velocity in x-direction at kth frame,
T = sampling interval,
q = number of scans since last measurement, and
α_x, β_x = fixed-coefficient filter parameters in x- and y-directions.

A usual initialization process for the filter is defined by

$$x_s(1) = x_p(1)x_o(1) \qquad \text{and} \qquad v_{sx}(1) = 0 \tag{4}$$

$$v_{sx}(2) = \frac{x_o(2) - x_o(1)}{T} \tag{5}$$

The foregoing equations are used for conditions under which an object is consistently detected. If the object is missed in a frame, the values of the coordinates are predicted as follows:

$$x_o(k) = x_s(k) = x_p(k) \qquad \text{and} \qquad v_{sx}(k) = v_{sx}(k-1) \tag{6}$$

The optimal relationship between α_x and β_x is known to be (*23*)

$$\beta_x = 2 \cdot (2 - \alpha_x) - 4\sqrt{1-\alpha_x} \tag{7}$$

The y-direction follows a set of equations similar to those shown earlier. Therefore, two-dimensional tracking can be fulfilled.

Extended Application of α-β-Filter

During execution of the algorithm shown in Figure 1, each input frame is first subtracted from the background. The regions (silhouettes) obtained from background subtraction are further filtered for size information. Then they are matched to existing objects. If no matching object is found, they are assigned as new ones. The matching process relies on a cost function that attempts to maintain the lowest cost for the correctly matched silhouette–object pair. Previously, the cost function was entirely based on inherent characteristics. The current version of PedTrack has the α-β-filter incorporated into this process. This filter allows the comparison of the predicted values for a particular object with those observed for each silhouette. The difference vector of a silhouette–object pair S_j and O_i is thus calculated as follows:

$$d(O_i, S_j) = \left(|A_i - A_j|, |H_i - H_j|, |W_i - W_j|, |G_i - G_j|, |\mathrm{PR}_i - P_j|\right) \tag{8}$$

where

A_i, A_j = silhouette–object areas,
H_i, H_j = heights,
W_i, W_j = widths,
G_i, G_j = grayscale histograms,
PR_i = object's predicted position, and
P_j = current position of silhouette to be matched to object.

The grayscale histogram difference $|G_i - G_j|$ is calculated as follows:

$$|G_i - G_j| = \sum_{k=0}^{255}\left|f_{k,O_i} - f_{k,S_j}\right| \tag{9}$$

where f_{k,O_i} and f_{k,S_j} are the frequencies for grayscale value k in the histogram of object i and silhouette j, respectively. In order to be able to compare the object and silhouettes, a cost is computed between each current object and its potential match. The cost function is the normalized difference of the parameter vectors of the silhouette–object pair, and it is calculated as follows:

$$c(O_i, S_j) = \sum_{n=1}^{4}\frac{d_n(O_i, S_j)}{R_n(O_i)} \tag{10}$$

where $d_n(O_i, S_j)$ is the nth element of $d(O_i, S_j)$ and $R_n(O_i)$ is the nth element of $R(O_i)$. $R(O_i)$ is the attribute vector of object O_i, which is calculated as follows:

$$R(O_i) = (A_i, H_i, W_i, G_i) \tag{11}$$

where

$$G_i = \sum_{k=0}^{255} f_{k,O_i} \tag{12}$$

By comparing predicted object positions and those of the current silhouette, the cost function can determine the relative movement of multiple objects. In this manner, the confusion between objects with different velocities can be reduced, for example, pedestrians crossing in opposing directions.

By integrating such a new tracking and matching approach into the previous system, a more robust PedTrack system is now presented. However, before this system is used, some configuration is necessary for collecting pedestrian movement data at intersections.

Detecting Pedestrian Movement

To detect pedestrian movements at intersections, a proper configuration of the PedTrack system should be made in advance. The idea of a waiting zone is proposed to collect pedestrian waiting time for crossing. The waiting zone not only provides additional restrictions on where the objects can be initialized but also further filters the incoming objects that are more likely to use the crosswalk. The proposed waiting zone is defined by a polygon at an entrance of a crosswalk in order to ensure that only pedestrian objects are initiated and tracked. The time the object spends in its initial waiting zone counts as time waited before crossing. Although the waiting time can be used to estimate pedestrian delay caused by the signal, the two may not always be identical. Pedestrian arrival rate and headway can be calculated by using the number of initialized objects in waiting zones over a time period and the recorded timestamps of the initializations.

For crossing-time data collection, two registration lines are configured to specify the beginning and end of pedestrian crossing movements. Once a pedestrian object crosses one registration line, a timer is started to count the crossing time of this object until the second registration line is crossed. The time an object spent between the two registration lines is defined as the crossing time for the object. For each pedestrian object, its path and time counts are displayed to show the progress of pedestrian crossing movements.

TESTING AND DATA RETRIEVAL

Study Sites

To obtain a variety of crossing characteristics and fully test the PedTrack system in diverse scenes, three signalized crossings were selected around the University of Washington in Seattle, where a large population of students resides. These three study sites are the Brooklyn crosswalk, the Campus Parkway crosswalk, and the 15th Avenue crosswalk.

The Brooklyn crosswalk (Figure 2*a*) is located at the southbound approach of Brooklyn Avenue Northeast next to Pacific Street. This crosswalk has relatively high bicyclist usage since it is a part of the Burke Gilman Trail biking corridor. As can be seen, the light post between the two registration lines makes observation of the scene more challenging. The Campus Parkway crosswalk (Figure 2*b*) is located at the eastbound approach of Northeast Campus Parkway. Several trolleybus routes pass by and create a complex scene with prolonged occlusions. The 15th Avenue crosswalk (Figure 2*c*) is located at the intersection of 15th Avenue Northeast and Northeast 41st Street. Trolleybus wires hanging over the street may create occlusions in addition to the occlusions caused by the buses themselves.

Waiting Zones

All the locations tested had an overhead angle view of the crosswalk to be examined. Such an overhead angle view helps reduce occlusion and obtain a broader observation of the entire crossing region and approaches. The three test sites together with the waiting zones and registration lines plotted for each crosswalk are shown in Figure 2.

Testing

Of the test locations, the Brooklyn crosswalk is the most favorable because of less frequent occlusions caused by large vehicles. The 15th Avenue crosswalk hosts numerous bus routes, and buses passing in front of the vantage point often block the entire intersection and create a total occlusion lasting throughout the entire crossing event. Thus, the Brooklyn crosswalk was tested for a total of 60 min, including morning, midday, and late afternoon sections. The other two sites were tested for 10 min each at midday. The detection and tracking rate of complete crossing events (waiting and completing the crossing from one registration line to another) was about 80%, providing sufficient data for analysis.

Figure 3 shows a complete crossing event. In Figure 3*a*, the arrival object is detected and initialized at the right waiting zone (as represented by the polygon in the upper-right corner of Figure 3*a*). Figure 3*b* displays the crossing stage of the event. The object has been registered at the right-hand registration line and is moving toward the left-hand registration line. Even though this object was occluded by the light post, it is still tracked through successfully. Finally, Figure 3*c* displays the completed crossing event; the tracked object has passed the left-hand registration line and its track has been cleared from the screen. As soon as a crossing event is complete, its crossing time is recorded. This sequence constitutes the necessary steps to obtain complete arrival, waiting, and crossing times for a pedestrian's approach–crossing movement.

Issues Encountered

As mentioned before, occlusion is a key issue in data collection. PedTrack can handle most occlusion issues, such as light posts and wires, to some extent. Figure 4 shows some of the typical occlusions encountered in the study sites. Figure 4*a* shows a complete occlusion resulting in a failure; the slow-moving bus blocked the object (and the crosswalk) completely for a significant portion of time, resulting in a miss of the pedestrian. Figure 4*b* shows a case of partial occlusion. PedTrack was successful in tracking the partially occluded object. This success shows the robustness of the proposed tracking algorithm. Through the field tests, vehicle–pedestrian, pedestrian–pedestrian, and pedestrian–static object occlusions were encountered, which are all challenging to video-based pedestrian detection and tracking. If

(a) (b) (c)

FIGURE 2 Crossing location setup for three test crosswalks: (*a*) Brooklyn Avenue Northeast, (*b*) Campus Parkway, and (*c*) 15th Avenue Northeast.

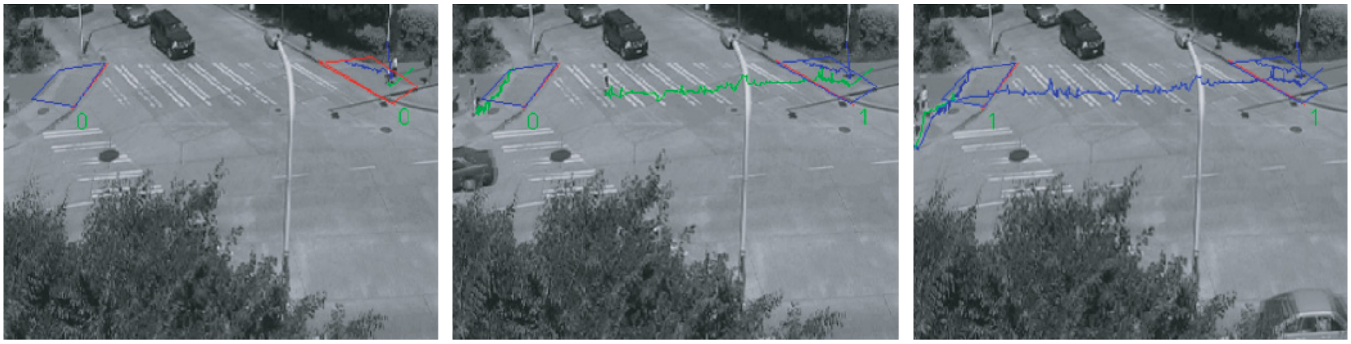

(a) (b) (c)

FIGURE 3 Complete crossing event: (*a*) object initiated, (*b*) object crossing, and (*c*) object data recorded.

two or more tracking objects move too close to each other, they are likely to merge into one composite object. An example of this type of occlusion can be seen in Figure 4*c*. As circled with a dashed line, a person–person occlusion occurred. PedTrack successfully reasoned between the two pedestrians and properly projected the movements of both pedestrians, although the upper pedestrian missed the left registration line by walking beyond the crosswalk marking. In this case, crossing time for this pedestrian will not be calculated and the crossing is considered incomplete.

PEDESTRIAN BEHAVIOR ANALYSIS

As described in the *Highway Capacity Manual* (HCM) 2000 (*24*), pedestrian characteristics are highly dependent on different factors, such as their activity areas. The 80-min long testing video sequence collected from three study sites contained 126 complete crossing events. From these 126 events, crossing times, waiting times, and arrival rates are analyzed and compared. These parameter analyses reveal distinctive movement characteristics of pedestrians and cyclists around the university district. Data associated with incomplete events, such as pedestrian waiting time, were not used because the intentions of the pedestrians could not be determined.

Crossing Time

The crossing time can be used to calibrate the green time for the pedestrian phase. The average crossing times for 15th Avenue Northeast, Campus Parkway, and Brooklyn Avenue Northeast were 9.2, 8.4, and 4.5 s, respectively. Brooklyn's short crossing time is probably best described as the result of a much higher cyclist percentage, as well as a shorter length. In Figure 5, it can be seen that the Brooklyn crossing data contain two peaks, one high peak at about 4 s and another, smaller peak at 10 s. The higher peak represents crossing times for bicyclists, and the lower peak represents regular pedestrian crossing times. This bimodal feature of crossing time enables further classification between pedestrians and bicyclists. However, it is important to note that although the average crossing time for bikes is shorter than that for pedestrians, the difference may vary depending on location and volume of bikes and pedestrians. Thus, more data are needed to implement this feature. The current version of PedTrack cannot distinguish pedestrians from bicycles. It is also worth mentioning that the overall average crossing time of 4.4 s could be misleading because it does not reflect the expected crossing time for pedestrians. Special attention must be paid when the PedTrack system is used to collect pedestrian crossing data for signal timing purposes.

Waiting Time

Along with the crossing time, waiting time is also an important measure for designing a signal timing plan and evaluating the performance of signalized intersections. If the delay, or average waiting time, is too long, the pedestrian's likelihood of violating the signal will increase. In fact, if the average delay is higher than 60 s, the likelihood of noncompliance will be very high, according to the HCM 2000 (*24*).

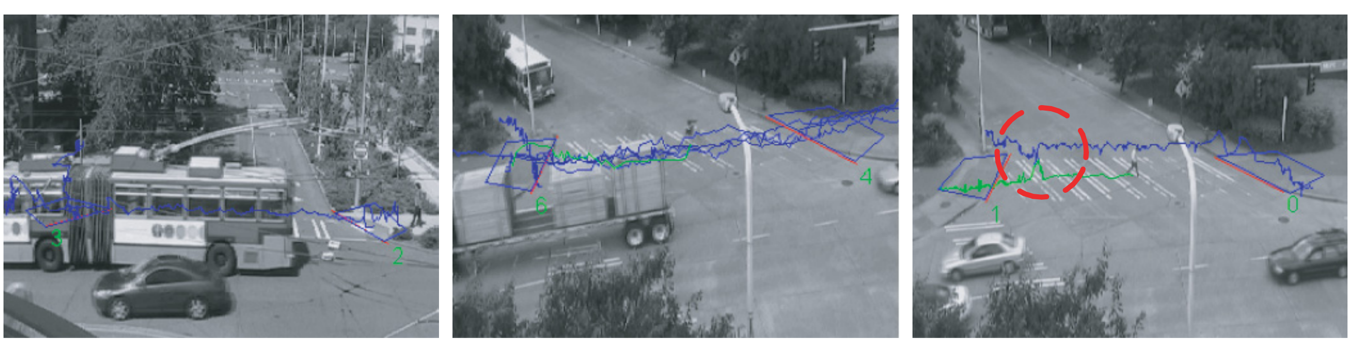

(a) (b) (c)

FIGURE 4 Various occlusion types: (*a*) complete occlusion, (*b*) partial occlusion, and (*c*) person–person occlusion.

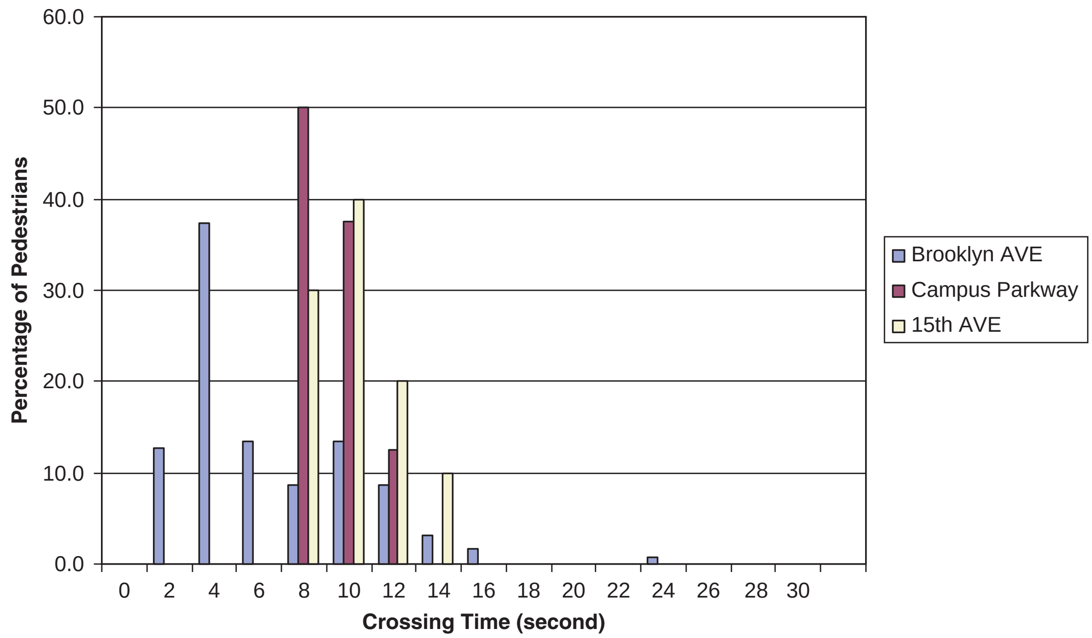

FIGURE 5 Crossing time statistics for each study site.

Figure 6 shows the waiting time distribution for each study site. The average waiting times for Brooklyn Avenue Northeast, 15th Avenue Northeast, and Campus Parkway are 1.4, 6.6, and 5.0 s, respectively. Brooklyn Avenue has the shortest waiting time, partly because of the long green time for the Brooklyn crosswalk. Most pedestrians are likely to arrive at the crosswalk during the green signal indication, resulting in a prompt crossing without a wait. Nevertheless, several extreme values obtained at other sites deserve further investigation in follow-up studies. For example, 30% of pedestrians at the 15th Avenue Northeast site waited more than 20 s. At the Campus Parkway site, 12.5% of pedestrians were waiting for 30 s, which is the exact length of the red phase of the pedestrian signal.

Arrival Rate

Arrival rate data have several important applications, such as predicting how many people will be queuing in a waiting zone, predicting expected delays, and calculating green time for the pedestrian phase. The pedestrian arrival rate depends on time of day. To investigate how

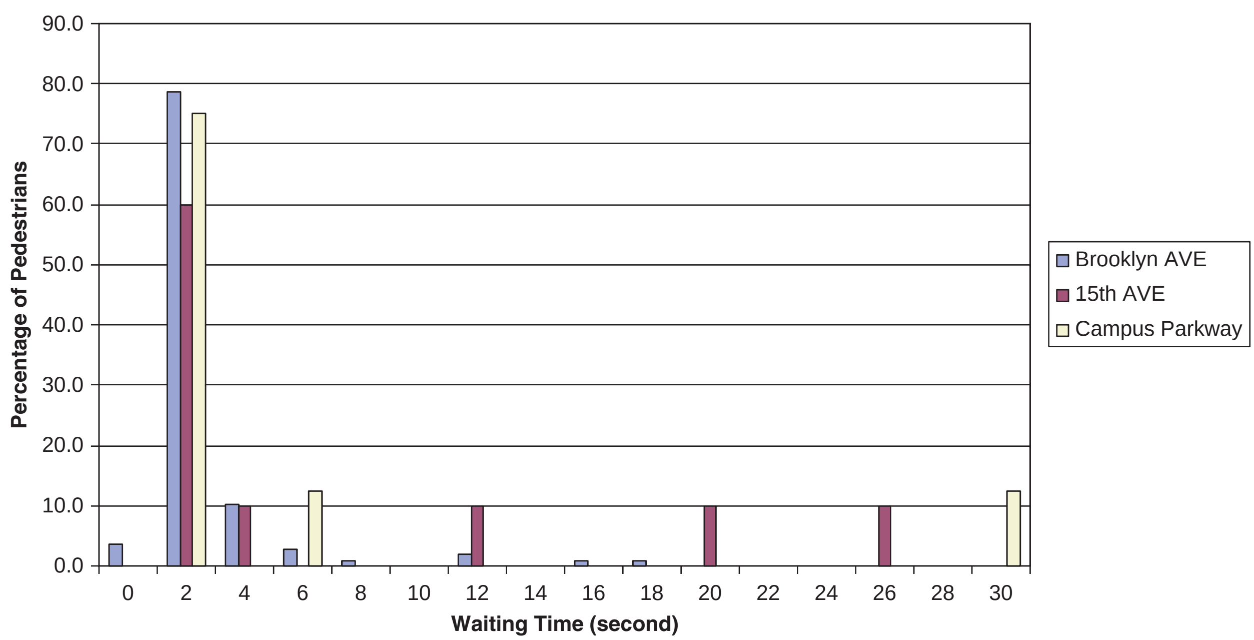

FIGURE 6 Waiting time statistics for each study site.

the pedestrian arrival rate changes with time of day, samples retrieved from the Brooklyn crosswalk were further divided into a morning group and an evening group. The results show that evening samples have a slightly lower arrival rate, 2.35 pedestrians per minute (p/m), than the morning rate, 2.78 p/m. However, these rates are still lower than the arrival rate at the 15th Avenue Northeast site, 6.93 p/m, and the one at the Campus Parkway site, 6.45 p/m. These two study sites are along major walking routes frequently used by students walking between the campus and residential areas.

SUMMARY

An automated computer-vision-based approach for real-time pedestrian detection and tracking is proposed. This proposed approach uses images from an ordinary uncalibrated video camera to detect complete crossing events at designated roadway sections. The waiting zone concept introduced here helps provide robust pedestrian tracking initialization and parameter extraction. The entire approach has been implemented and tested at three signalized crosswalks near the University of Washington campus. About 80% of pedestrians and cyclists were successfully detected and tracked at the three challenging study sites. PedTrack proved its potential to be a feasible alternative to manual pedestrian data collection.

With the pedestrian crossing data recorded by the system, several statistical analyses were conducted to demonstrate how PedTrack can help traffic engineering practice and research. Pedestrian waiting time, crossing time, and arrival rate data collected by PedTrack are potentially valuable inputs for intersection geometric design, signal timing, and safety studies.

However, the system is still in its early research and development stage. Much work needs to be done to make it a practical tool for automatic pedestrian data collection. Further enhancements in the detection and tracking algorithm will definitely help improve the accuracy of the proposed approach. PedTrack serves as a practical example that shows how video image processing can help collect data automatically for traffic engineering practice and research.

REFERENCES

1. Transportation Equity Act for the 21st Century (TEA-21). U.S. Department of Transportation. http://www.fhwa.dot.gov/tea21/. Accessed July 30, 2007.
2. *Bicycle and Pedestrian Data: Sources, Needs and Gaps.* Bureau of Transportation Statistics, U.S. Department of Transportation, June 1998.
3. Pushkarev, B., and J. Zupan. *Urban Space for Pedestrians.* MIT Press, Cambridge, Mass., 1975.
4. Gates, T. J., D. A. Noyce, A. R. Bill, and N. Van Ee. Recommended Walking Speeds for Timing of Pedestrian Clearance Intervals Based on Characteristics of the Pedestrian Population. In *Transportation Research Record: Journal of the Transportation Research Board, No. 1982,* Transportation Research Board of the National Academies, Washington, D.C., 2006, pp. 38–47.
5. Zhang, G., R. P. Avery, and Y. Wang. A Video-Based Vehicle Detection and Classification System for Real-Time Traffic Data Collection Using Uncalibrated Video Cameras. In *Transportation Research Record: Journal of the Transportation Research Board, No. 1993,* Transportation Research Board of the National Academies, Washington, D.C., 2007, pp. 138–147.
6. Gupte, S., O. Masoud, R. F. K. Martin, and N. P. Papanikolopoulos. Detection and Classification of Vehicles. *IEEE Transactions on Intelligent Transportation Systems,* Vol. 3, No. 1, 2002, pp. 37–47.
7. Rad, R., and M. Jamzad. Real Time Classification and Tracking of Multiple Vehicles in Highways. *Pattern Recognition Letters,* Vol. 26, No. 10, 2005, pp. 1597–1607.
8. Avery, R. P., G. Zhang, Y. Wang, and N. L. Nihan. Investigation into Shadow Removal from Traffic Images. In *Transportation Research Record: Journal of the Transportation Research Board, No. 2000,* Transportation Research Board of the National Academies, Washington, D.C., 2007, pp. 70–77.
9. Avery, R. P., Y. Wang, and G. S. Rutherford. Length-Based Vehicle Classification Using Images from Uncalibrated Video Cameras. *Proc., 7th International Conference on Intelligent Transportation Systems,* IEEE, New York, Oct. 2004, pp. 737–742.
10. SRF Consulting Group, Inc., and Minnesota Department of Transportation. *Bicycle and Pedestrian Detection: Final Report.* FHWA, U.S. Department of Transportation, 2003.
11. Noyce, D. A., A. Gajendran, and R. Dharmaraju. Development of a Bicycle and Pedestrian Detection and Classification Algorithm for Active-Infrared Overhead Vehicle Imaging Sensors. In *Transportation Research Record: Journal of the Transportation Research Board, No. 1982,* Transportation Research Board of the National Academies, Washington, D.C., 2006, pp. 202–209.
12. Hughes, R., H. Huang, C. Zegeer, and M. Cynecki. *Evaluation of Automated Pedestrian Detection at Signalized Intersections.* Publication FHWA-RD-00-097. FHWA, U.S. Department of Transportation, 2001.
13. Malinovskiy, Y., J. Zheng, and Y. Wang. Simple and Model-Free Algorithm for Real-Time Pedestrian Detection and Tracking. Presented at the 86th Annual Meeting of the Transportation Research Board, Washington, D.C., 2007.
14. Abramson, Y., and B. Steux. Hardware-Friendly Pedestrian Detection and Impact Prediction. *IEEE Intelligent Vehicles Symposium,* 2004, pp. 590–595.
15. Satoh, Y., T. Okatani, and K. Deguchi. A Color-Based Probabilistic Tracking by Using Graphical Models. *Proc., 2004 Conference on Intelligent Robots and Systems,* Vol. 1, 2004, pp. 631–636.
16. Tissainayagam, P., and D. Suter. Assessing the Performance of Corner Detectors for Point Feature Tracking Applications. *Image and Vision Computing,* Vol. 22, No. 8, 2004, pp. 663–679.
17. Munder, S., and D. M. Gavrila. An Experimental Study on Pedestrian Classification. *IEEE Transactions on Pattern Analysis and Machine Intelligence,* Vol. 28, No. 11, 2006, pp. 1863–1868.
18. Gavrila, D. M., and S. Munder. Multi-Cue Pedestrian Detection and Tracking from a Moving Vehicle. *International Journal of Computer Vision,* Vol. 73, No. 1, 2007, pp. 41–59.
19. Zheng, J., Y. Wang, N. L. Nihan, and M. E. Hallenbeck. Detecting Cycle Failures at Signalized Intersections Using Video Image Processing. *Computer-Aided Civil and Infrastructure Engineering,* Vol. 21, No. 6, 2006, pp. 425–435.
20. Sheikh, Y., Y. Zhai, K. Shafique, and M. Shah. Visual Monitoring of Railroad Grade Crossing. *Proceedings of SPIE,* Vol. 5403, No. 1, 2004, pp. 654–660.
21. Masoud, O., and N. P. Papanikolopoulos. A Novel Method for Tracking and Counting Pedestrians in Real-Time Using a Single Camera. *IEEE Transactions on Vehicular Technology,* Vol. 50, No. 5, 2001, pp. 1267–1278.
22. Blackman, S. S. *Multiple-Target Tracking with Radar Applications.* Artech House, Inc., Norwood, Mass., 1986.
23. Kalata, P. R. The Tracking Index: A Generalized Parameter for α-β and α-β-γ Target Trackers. *IEEE Transactions on Aerospace and Electronic Systems,* Vol. AES-20, No. 6, 1984, pp. 174–182.
24. *Highway Capacity Manual.* TRB, National Research Council, Washington, D.C., 2000.

The Pedestrians Committee sponsored publication of this paper.